PHARMACOLOGY

Aβ oligomers induce pathophysiological mGluR5 signaling in Alzheimer's disease model mice in a sex-selective manner

Khaled S. Abd-Elrahman[1,2,3]*, Awatif Albaker[1,2,4]*, Jessica M. de Souza[1,2,5], Fabiola M. Ribeiro[5], Michael G. Schlossmacher[1,2,6,7], Mario Tiberi[1,2,6,7,8], Alison Hamilton[1,2†], Stephen S. G. Ferguson[1,2†‡]

The prevalence, presentation, and progression of Alzheimer's disease (AD) differ between men and women, although β-amyloid (Aβ) deposition is a pathological hallmark of AD in both sexes. Aβ-induced activation of the neuronal glutamate receptor mGluR5 is linked to AD progression. However, we found that mGluR5 exhibits distinct sex-dependent profiles. Specifically, mGluR5 isolated from male mouse cortical and hippocampal tissues bound with high affinity to Aβ oligomers, whereas mGluR5 from female mice exhibited no such affinity. This sex-selective Aβ-mGluR5 interaction did not appear to depend on estrogen, but rather Aβ interaction with cellular prion protein (PrP^C), which was detected only in male mouse brain homogenates. The ternary complex between mGluR5, Aβ oligomers, and PrP^C was essential to elicit mGluR5-dependent pathological suppression of autophagy in primary neuronal cultures. Pharmacological inhibition of mGluR5 reactivated autophagy, mitigated Aβ pathology, and reversed cognitive decline in male APPswe/PS1ΔE9 mice, but not in their female counterparts. Aβ oligomers also bound with high affinity to human mGluR5 isolated from postmortem donor male cortical brain tissue, but not that from female samples, suggesting that this mechanism may be relevant to patients. Our findings indicate that mGluR5 does not contribute to Aβ pathology in females, highlighting the complexity of mGluR5 pharmacology and Aβ signaling that supports the need for sex-specific stratification in clinical trials assessing AD therapeutics.

INTRODUCTION

Alzheimer's disease (AD) is a progressive neurodegenerative disease characterized by age-related memory loss and cognitive decline, and despite the alarming prevalence, no treatments currently exist to either modify or reverse its progression (*1*–*3*). β-Amyloid (Aβ) oligomers and hyperphosphorylated tau protein, which represent pathological hallmarks of AD, accumulate with disease progression, disrupt neuronal signaling, and trigger neurodegeneration (*4*–*6*). Sex is an important modulator of AD prevalence; both clinical and preclinical evidence indicate that the incidence in females is higher than in age- and risk factor–matched males (*7*–*10*). This higher incidence of cognitive impairment is commonly attributed to reduced estrogen and/or estrogen receptor levels after menopause (*11*–*13*). However, this assumption has been weakened by a large-scale clinical study (the Women's Health Initiative Memory Study) demonstrating rather an increased risk of dementia and poor cognitive outcomes after hormone replacement therapy (*14*, *15*).

Glutamate, the main excitatory brain neurotransmitter, plays a key role in learning and memory, and the $G_{\alpha q}$-coupled metabotropic glutamate receptor 5 (mGluR5) is of particular interest in AD pathology (*5*, *16*). mGluR5 functions as an extracellular scaffold for Aβ and cellular prion protein (PrP^C), and the complex between PrP^C and mGluR5 is essential for Aβ binding (*17*–*19*). Aβ also promotes mGluR5 clustering, increases intracellular Ca^{2+} release, and inhibits autophagy (*17*, *19*, *20*). Moreover, the pharmacological and genetic silencing of mGluR5 reverses cognitive deficits and reduces Aβ pathology in male AD rodent models (*20*–*24*). Although these studies emphasized the key role of mGluR5 in AD pathophysiology, it is not yet clear whether alterations in mGluR5 signaling are conserved between male and female AD models. Given that both clinical and experimental evidence indicate a divergent AD pathology between males and female, the marked drug treatment failure rate in AD clinical trials warrants a better delineation of the molecular signaling mechanism(s) underlying sex-related pathophysiological differences in AD (*7*, *10*). It is also important to note that some previous studies have pharmacologically targeted mGluR5 in AD mice from both sexes, but unexpectedly, the results were not stratified according to sex, and therefore, an accurate representation for the contribution of pathological mGluR5 signaling to AD in females could not be reached (*25*, *26*).

In this study, we aimed to assess whether mGluR5 differentially contributes to pathology in both sexes, and therefore, we evaluated the binding affinity of Aβ to mGluR5 and the efficacy of Aβ in triggering pathological autophagic signaling in male and female AD mice. We also tested whether the orally bioavailable, negative allosteric modulator (NAM) of mGluR5, 2-chloro-4-((2,5-dimethyl-1-(4-(trifluoromethoxy)phenyl)-1*H*-imidazol-4-yl)ethynyl) pyridine (CTEP) (*27*), differentially alters cognition and progression of Aβ pathology between male and female APPswe/PS1ΔE9 (APP) mice (*28*). It is worth noting that other mGluR5 ligands have been reported to

[1]University of Ottawa Brain and Mind Research Institute, Ottawa, Ontario K1H 8M5, Canada. [2]Department of Cellular and Molecular Medicine, University of Ottawa, Ottawa, Ontario K1H 8M5, Canada. [3]Department of Pharmacology and Toxicology, Faculty of Pharmacy, Alexandria University, Alexandria 21521, Egypt. [4]Department of Pharmacology and Toxicology, College of Pharmacy, King Saud University, Riyadh 12371, Saudi Arabia. [5]Department of Biochemistry and Immunology, ICB, Universidade Federalde Minas Gerais, Belo Horizonte 31270-901, Brazil. [6]Department of Medicine, University of Ottawa, Ottawa, Ontario K1H 8M5, Canada. [7]Neuroscience Program, Ottawa Hospital Research Institute, Ottawa, Ontario, K1H 8L6, Canada [8]Department of Psychiatry, University of Ottawa, Ottawa, Ontario K1H 8M5, Canada.
*These authors contributed equally to this work.
†These authors contributed equally as co-senior authors.
‡Corresponding author. Email: sferguso@uottawa.ca

improve either only memory deficits (namely, BMS-984923) or only Aβ pathological signaling (namely, CDPPB) in AD mouse models (*25*, *26*). Our choice of CTEP was based on its reportedly superior capabilities in reversing Aβ pathology and improving cognitive function with no evidence of drug-related adverse outcomes after extended treatment regimens (*22*, *24*).

Our findings reveal that mGluR5 exhibits unexpected and distinct pharmacological profiles with respect to Aβ oligomer and PrP^C interactions in male and female brain tissue that can dictate the relative contribution of mGluR5 to AD pathology and, hence, therapeutic efficacy of mGluR5 NAM between both sexes.

RESULTS

Sex-specific interaction of Aβ oligomers and PrP^C with mGluR5 in mouse brain

Aβ oligomers bind with high affinity to the PrP^C/mGluR5 complex, thereby driving the pathological signaling of mGluR5 (*17*, *29*). Therefore, we first tested whether the binding of Aβ oligomers to endogenous mGluR5 is sex specific. We assessed Aβ oligomer–mediated displacement of radiolabeled mGluR5 antagonist [2-methyl-6-(phenylethynyl)-pyridine (MPEP)] binding to endogenously expressed mGluR5 in plasma membrane preparations from male and female wild-type mouse cortex and hippocampus. To our surprise, Aβ oligomers effectively displaced [^{3}H]-MPEP binding to male, but not female, mGluR5 in mouse cortical (Fig. 1, A and B, and table S1) and hippocampal membrane preparations (Fig. 1, C and D, and table S1). The nonradioactive MPEP displaced [^{3}H]-MPEP binding in a biphasic manner, and the curves were not different when both sexes were compared in each brain regions (Fig. 1, A to D, and table S1). Treatment of female mice with the estrogen antagonist ICI 182,780 for 2 weeks did not change either Aβ or MPEP displacement curves in cortical membrane preparations, indicating that altered Aβ binding to mGluR5 in female mouse brain was estrogen independent (Fig. 1E and table S1). Together, Aβ oligomer–binding assays revealed previously unknown distinct sex-dependent pharmacological profiles for mGluR5.

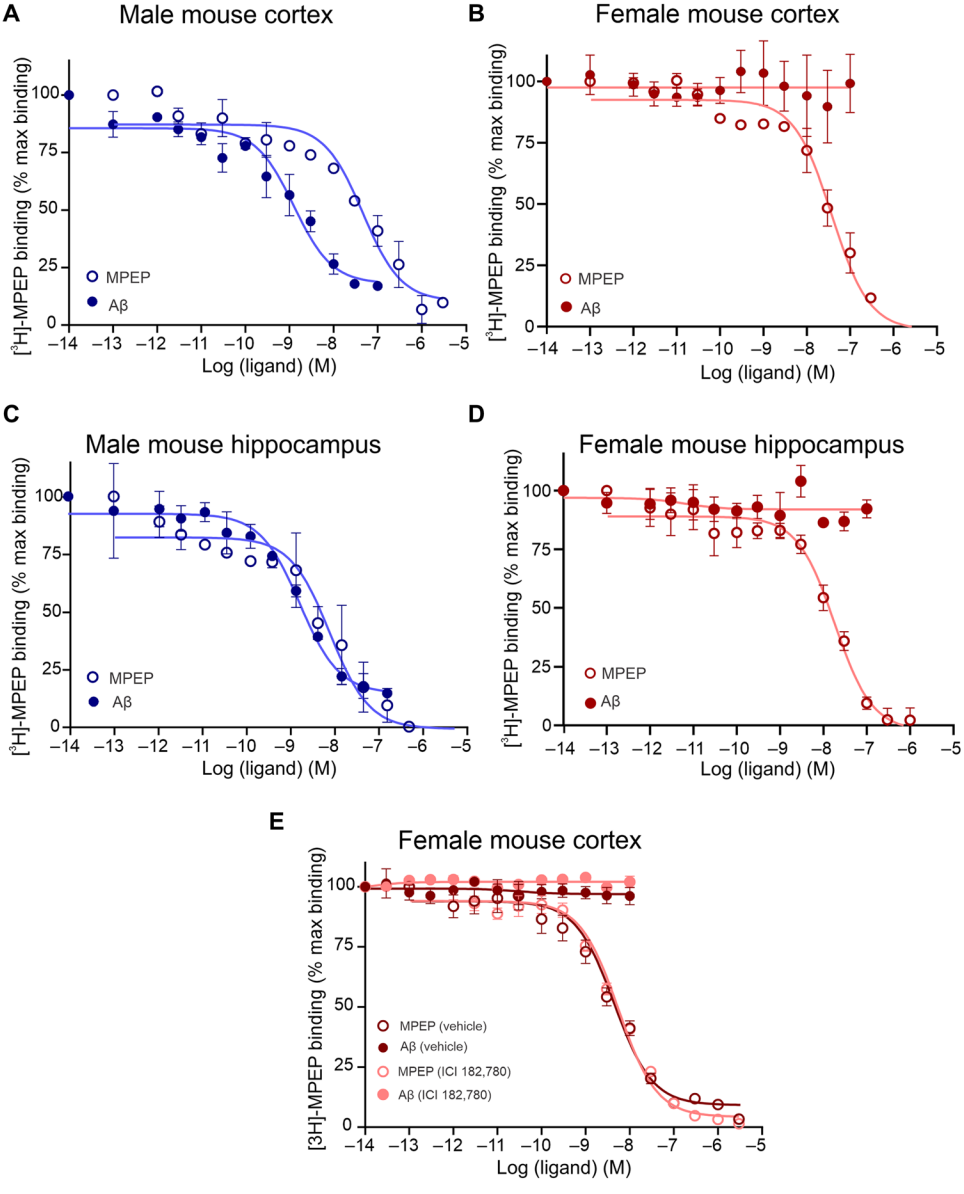

Fig. 1. Sex-specific binding of Aβ oligomers to mGluR5 in mouse brain. (**A** to **E**) [^{3}H]-MPEP displacement curves for MPEP and Aβ oligomers in membrane preparations from wild-type (A) male mouse cortex, (B) female mouse cortex, (C) male mouse hippocampus, (D) female mouse hippocampus, and (E) female mouse cortex after treatment with ICI 182,780 or vehicle. Each binding curve represents the mean ± SEM of technical duplicates from three to four mice in each group.

Because Aβ oligomers binding to mGluR5 is known to be dependent on the interaction of the receptor with PrP^C (*17*, *29*–*31*), we tested whether PrP^C interacts with mGluR5 in a sex-specific manner. We first confirmed that the size of the Aβ oligomers that we used in our study is capable of interacting with mGluR5/PrP^C scaffold and that PrP^C is key for Aβ binding to mGluR5 by performing radioligand binding assays in PrP^C null (CF10) cells transfected with mGluR5. In control experiments, we found that Aβ oligomers did not displace [^{3}H]-MPEP binding in CF10 cells (Fig. 2A), but that cotransfection of CF10 cells with PrP^C restored the ability of Aβ oligomer to bind mGluR5 (Fig. 2B). We then tested whether PrP^C binding to mGluR5 was different between both sexes and found that mGluR5 coimmunoprecipitated with PrP^C from male, but not from female, wild-type mouse hippocampal tissue (Fig. 2C and fig. S1). Binding specificity of PrP^C antibody to mGluR5 was validated by the

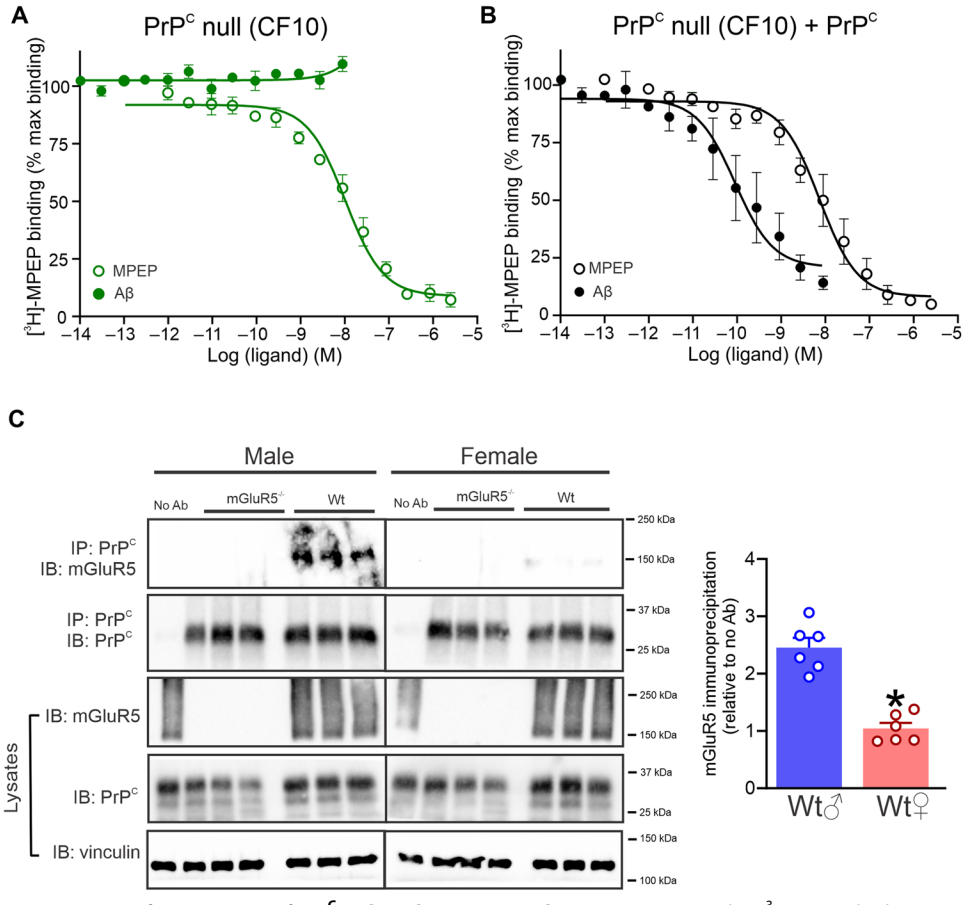

Fig. 2. Sex-specific interaction of PrP^C with mGluR5 in mouse hippocampus. (**A** and **B**) [^{3}H]-MPEP displacement curves for MPEP and Aβ oligomers in membrane preparations from CF10 cells transfected with FLAG-mGluR5 (A) or FLAG-mGluR5 + PrP^C (B). Each binding curve represents the mean ± SEM of three independent duplicate experiments. (**C**) Representative immunoblot (IB) and quantification of mGluR5 coimmunoprecipitated with PrP^C (IP) from male and female wild-type (Wt) hippocampus with corresponding lysates and loading control. Hippocampal tissue from male and female $mGluR^{-/-}$ or Wt mice in the absence of PrP^C antibody (no Ab) served as a negative control. Samples from male and female hippocampus were probed on the same blot for each protein. mGluR5 immunoprecipitation in male and female wild-type hippocampus was normalized to corresponding lysates and is presented relative to the no Ab lane of each sex ($n = 6$ mice per group). *$P < 0.05$ versus male values assessed by unpaired Student's t test.

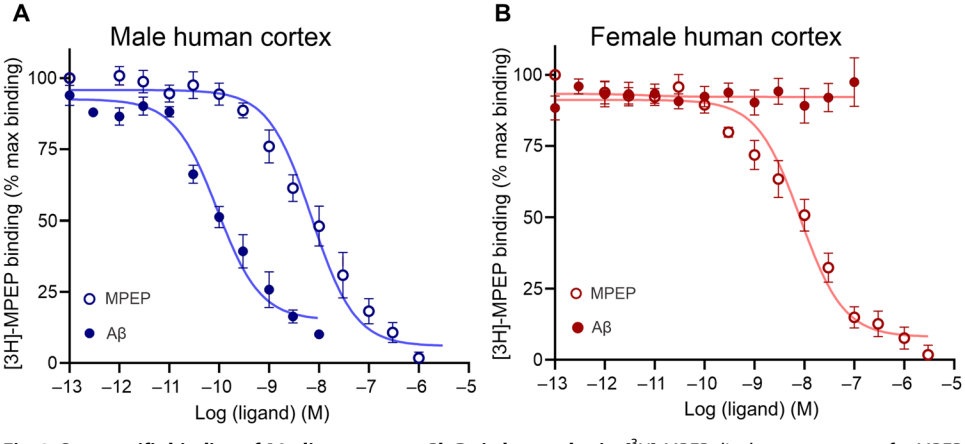

Fig. 3. Sex-specific binding of Aβ oligomers to mGluR5 in human brain. [^{3}H]-MPEP displacement curves for MPEP and Aβ oligomers in membrane preparations from (**A**) male and (**B**) female human cortex. Each binding curve represents the mean ± SEM of technical duplicates from four to five subjects in each group.

lack of receptor immunoprecipitation in hippocampus from $mGluR5^{-/-}$ mice. Overall, our findings indicated that, unlike what was observed for males, the mGluR5/Aβ oligomer/PrP^C ternary complex is not formed in female mouse brain.

Sex-specific binding of Aβ oligomers to mGluR5 in human cortex

To validate that sex-specific binding of Aβ to mGluR5 was not exclusive to mouse tissues, we performed [^{3}H]-MPEP binding displacement assays in cortical membranes prepared from male and female human cortical brain samples obtained at autopsy. Identical to what was observed for mouse cortical membranes, displacement of [^{3}H]-MPEP binding by MPEP was not significantly different between male and female human cortical membranes (Fig. 3, A and B, and table S1). However, Aβ oligomers only displaced [^{3}H]-MPEP binding to male membranes (Fig. 3, A and B, and table S1), suggesting that the differential binding of Aβ oligomers to mGluR5 between males and females is an evolutionally conserved phenomenon and may contribute to sex-specific pathophysiology in human patients with AD.

Sex-specific Aβ-activated mGluR5 signaling in primary embryonic neuronal cultures

Because Aβ oligomers binding to mGluR5 was shown to induce receptor clustering and activate its pathological signaling (*17*, *19*), we tested whether Aβ oligomer binding to mGluR5 could inactivate the glycogen synthase kinase 3β (GSK3β)–ZBTB16 autophagy pathway, which we identified to be engaged downstream of mGluR5, in a sex-specific manner in the absence of sex hormones in the media. The GSK3β-ZBTB16 pathway was one of the mGluR5 autophagic signaling mechanisms that was previously observed to be dysregulated in male AD mouse models and correlated with a loss of clearance of Aβ (*20*, *24*, *32*). Thus, to avoid potentially confounding influence of sex hormones on mGluR5 signaling, we examined Aβ-evoked signaling in primary cortical neurons isolated from wild-type male and female embryonic day 15 (E15) mice. Sex of the cultures was determined by polymerase chain reaction (PCR) amplification to

detect X chromosome–linked *Rbm31* gene relative to its divergent Y chromosome gametolog (*33*) (Fig. 4A). Treatment of male cultures with Aβ oligomers (100 nM) induced the phosphorylation of GSK3β at Ser^9, increased ZBTB16 expression, and inhibited autophagy as measured by increased p62 expression in a manner that was inhibited by CTEP (10 μM; Fig. 4B and fig. S2). These changes were not observed in cultures derived from female embryos (Fig. 4B and fig. S2). Our results clearly demonstrated that Aβ oligomers inactivated ZBTB16 autophagic signaling in male, but not in female, neurons in a sex hormone–independent but mGluR5-dependent manner.

mGluR5 inhibition reduced AD-related pathology in male, but not in female, APP mice

We determined whether the differences in mGluR5-regulated GSK3β-ZBTB16 signaling between male and female cultured neurons after exposure to Aβ oligomers were translatable in vivo. To test this, 6-month-old male and female wild-type and APP mice were treated with vehicle or CTEP (2 mg/kg) for 12 weeks, and brains were harvested at the end of treatment for biochemical and immunohistochemical assessments. We chose the APP model because both male and female mice exhibited a robust Aβ accumulation and cognitive impairment by 9 months (*28*, *34*, *35*), and this treatment regime was effective in improving memory deficits and reversing Aβ pathology in 12-month-old male APP mice (*22*). Here, we found that the activity or expression of cell signaling mediators of the autophagic GSK3β-ZBTB16-ATG14 pathway was inhibited in male APP mice. Specifically, we detected increased $pSer^9$-GSK3β level, increased ZBTB16 expression, and accumulation of p62 protein (Fig. 5, A to D, and fig. S3) (*20*, *32*, *36*). CTEP treatment of male APP mice attenuated $pSer^9$-GSK3β phosphorylation, reduced ZBTB16 protein expression, and increased ATG14 protein expression that coincided with a loss of p62 protein (Fig. 5, A to D, and fig. S3). In contrast, no alterations in GSK3β-ZBTB16-ATG14 signaling were observed in vehicle-treated female APP mice, and, as a consequence, CTEP treatment had no discernable effect on the GSK3β-ZBTB16-ATG14 pathway in either wild-type or APP female mice (Fig. 5, A to D, and fig. S3). Female wild-type and APP mouse brains presented with lower $pSer^9$-GSK3β compared with male wild type, an observation that was reported to unfold in female mouse brain at the age of 6 months and later and was likely attributed to age-dependent changes in hormone levels (*37*).

We then tested whether the sex-specific effect of CTEP on GSK3β-ZBTB16-ATG14 signaling in APP mice was correlated with a similar change in Aβ pathology. We found that the deposition of Aβ plaque density was significantly reduced in male APP mice after the CTEP treatment regime, whereas Aβ plaque density in either the hippocampus or cortex of female APP animals was not changed in response to CTEP treatment (Fig. 5, E and F). Soluble Aβ levels detected in brain lysates from both vehicle-treated male and female APP mice were comparably increased versus

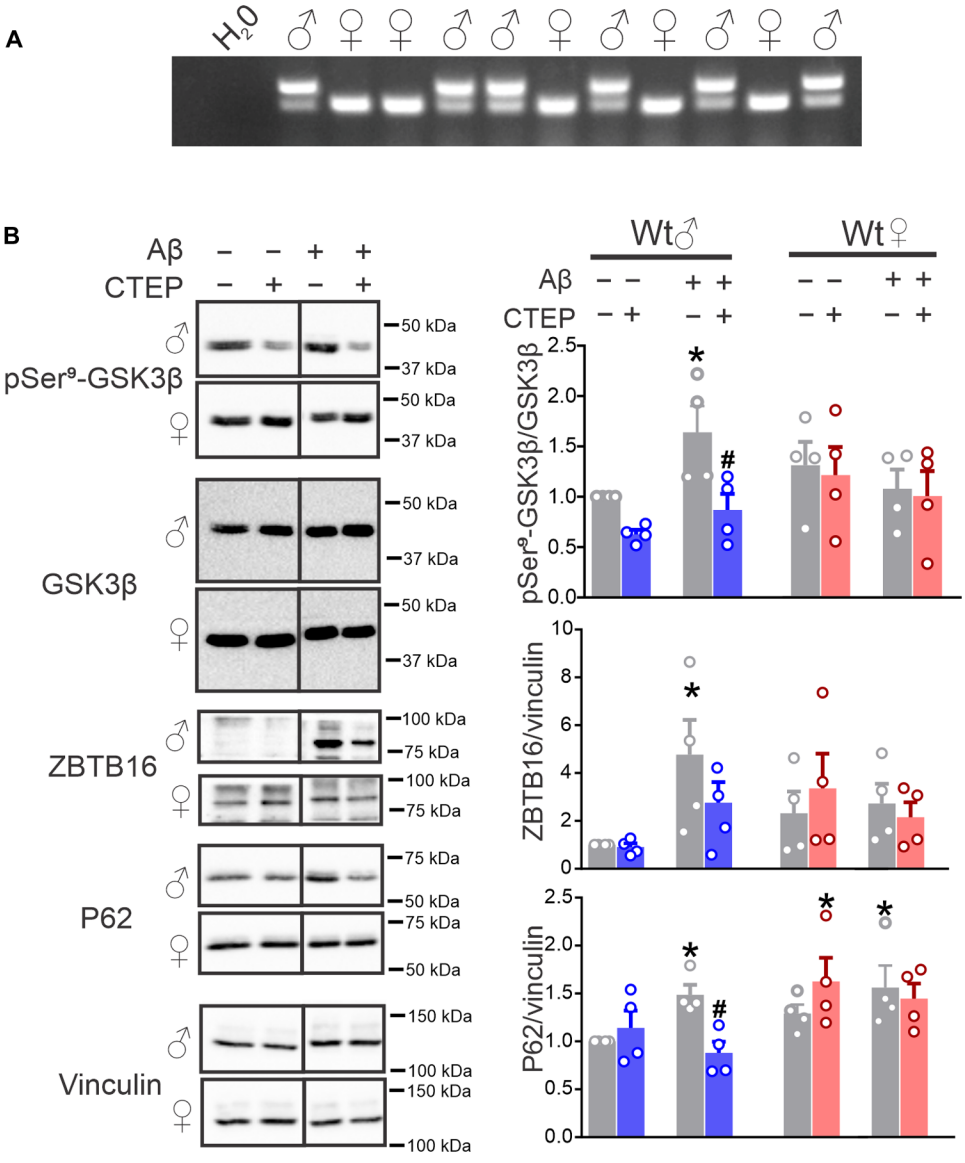

Fig. 4. Sex-specific Aβ oligomer–mediated activation of mGluR5 signaling in mouse neuronal cultures. (**A**) Representative gel for the *Rbm31* gene PCR amplicon in male and female E15 Wt mouse embryos. (**B**) Representative immunoblots and quantification of $pSer^9$-GSK3β, ZBTB16, and p62 normalized to loading controls or total protein and expressed as a fraction of the nontreated male cultures in primary cultured cortical neurons from male and female Wt E15 embryos treated with Aβ oligomers (100 nM) in the absence (DMSO) or presence of CTEP (10 μM). Data represent means ± SEM ($n = 4$ cultures per group). Samples from male and female cultures were probed on the same blot for each protein. $^*P < 0.05$ versus nontreated male cultures and $^{\#}P < 0.05$ versus Aβ-treated male cultures assessed by three-way ANOVA and Fisher's least significant difference (LSD) comparisons.

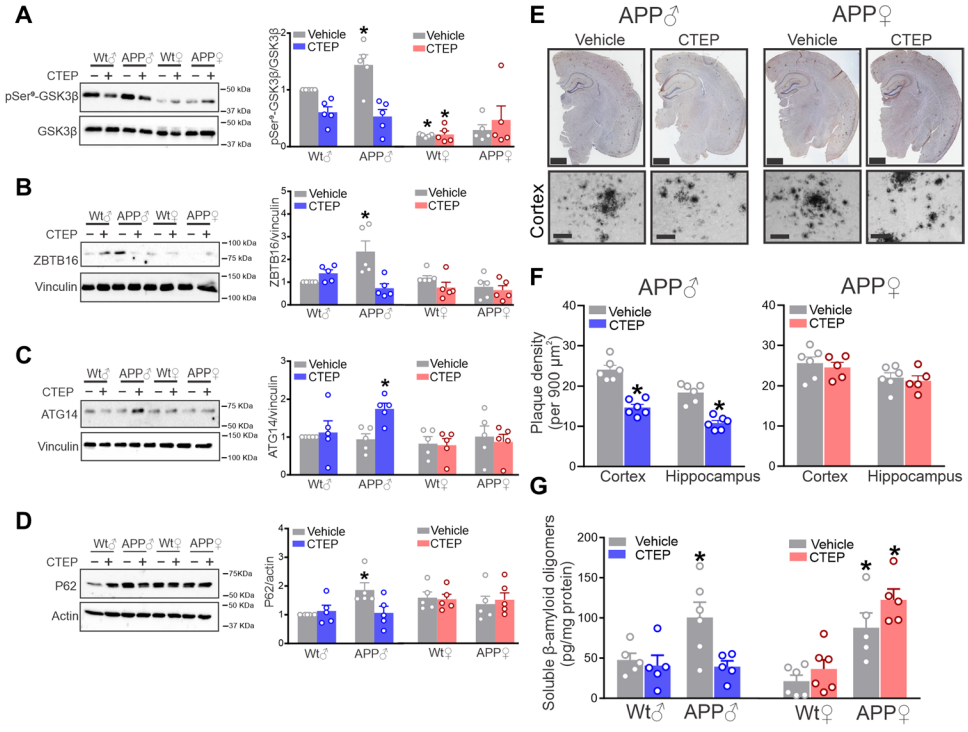

Fig. 5. CTEP activates autophagy and reduces Aβ pathology in male, but not in female, APP mice. (**A** to **D**) Representative immunoblots and quantification of (A) pSer^9-GSK3β, (B) ZBTB16, (C) ATG14, and (D) p62 with the corresponding loading controls or total protein from brain lysates of 6-month-old male and female Wt and APP mice treated with vehicle or CTEP (2 mg/kg) for 12 weeks. Data are means ± SEM ($n = 5$ mice per group), quantified relative to vehicle-treated male Wt mice values. (**E** and **F**) Representative images of Aβ staining in whole-brain slice and magnified area of cortex (E) and plaque density in hippocampal and cortical slices (F) from mice described in (A) to (D), each quantified in five different 900-μm^2 regions from six brain slices per mouse. Scale bars, 1 mm for whole slices and 50 μm for cortex. (**G**) Aβ oligomer concentrations (pg/mg) in tissue from mice described in (A) to (D). *$P < 0.05$ versus vehicle-treated male Wt values assessed by three-way ANOVA and Fisher's LSD comparisons (B to D and G) or Kruskal-Wallis tests (A) or versus vehicle-treated same-sex APP assessed by two-way ANOVA and Bonferroni-corrected *t* tests (F).

sex-matched wild-type mice (Fig. 5G). CTEP treatment of male APP mice resulted in significantly reduced soluble Aβ levels, whereas it did not change soluble Aβ levels in female APP mice (Fig. 5G). Overall, these findings show that, although Aβ oligomers contribute to AD-like neuropathology in both sexes of APP mice, the Aβ oligomer–mediated antagonism of an mGluR5-regulated, GSK3β-ZBTB16–mediated autophagy that contributes to AD-like pathology was exclusive to male mice. This may explain why mGluR5 inhibition reduced Aβ deposition in male APP mice only.

mGluR5 blockade improved cognitive deficits in male, but not in female, APP mice

We then tested whether sex-specific outcomes of CTEP treatment on Aβ pathology were reflected on the memory function of APP mice. Vehicle- and CTEP-treated male and female wild-type and APP mice were tested for impairments in working and spatial memory using the novel object recognition test, the Morris water maze (MWM) test, and MWM with reversal (RMWM) test. In the novel object recognition test, vehicle-treated wild-type male and female mice discriminated between novel and familiar objects, whereas vehicle-treated male and female APP mice failed to discriminate between objects (Fig. 6, A and B). After CTEP treatment, male APP mice regained the capacity to discriminate between objects, whereas female APP mice remained cognitively impaired (Fig. 6, A and B). In MWM and RMWM, vehicle-treated male and female APP mice exhibited significantly longer escape latencies and less time spent in target quadrant than did similarly treated same-sex wild-type mice (Fig. 7, A to D). CTEP treatment improved male APP mice performance in both the MWM and RMWM as measured by shorter escape latency and longer time spent in target quadrant with values indistinguishable from wild-type mice (Fig. 7, A to D). In contrast, when compared with vehicle-treated female APP mice, CTEP treatment did not improve either escape latency or time spent in target quadrant of female APP mice in either the MWM or RMWM (Fig. 7, A to D). Unlike what we observed for wild-type male mice, CTEP treatment impaired female wild-type mouse performance in the RMWM compared with vehicle-treated wild-type mice, with the mice showing impaired escape latencies and reduced time spent in the target quadrant (Fig. 7, C and D). The latter observation further confirms a key fundamental difference in mGluR5 pharmacology between both sexes that warrants further investigation. Together, the data indicate that male and female APP mice can have comparable cognitive impairments and similar Aβ burdens, but that chronic inhibition of mGluR5 mitigates AD-like neuropathology only in male mice. These results corroborate our primary neuronal culture findings, described above, and provide in vivo evidence for the sex-specific contribution of mGluR5 to AD pathophysiology.

DISCUSSION

A challenge in AD therapy is identification of pharmaceutical targets that mitigate both disease symptomology and pathology. Genetic and pharmacological silencing of mGluR5 identifies its key role in mediating Aβ-related cognitive decline and pathology in male AD mice (*21*, *22*, *24*). However, gender-specific responses to therapies are reported in AD and other neurological diseases, which complicates the process of drug discovery (*7*, *8*, *10*). We found here that, unlike what is observed in male mouse, mGluR5 is incapable of scaffolding either Aβ oligomers or PrP^C in the female mouse brain to elicit pathological mGluR5 signaling (Fig. 8). This failure to form a mGluR5-scaffolded complex is conserved in both mouse and human female cortex and represents an unexpected sex-specific regulation of mGluR5 pharmacology. The sex-dependent contribution of mGluR5 to AD pathology was validated in vivo, wherein treatment of APP mice with an mGluR5 NAM improved cognitive

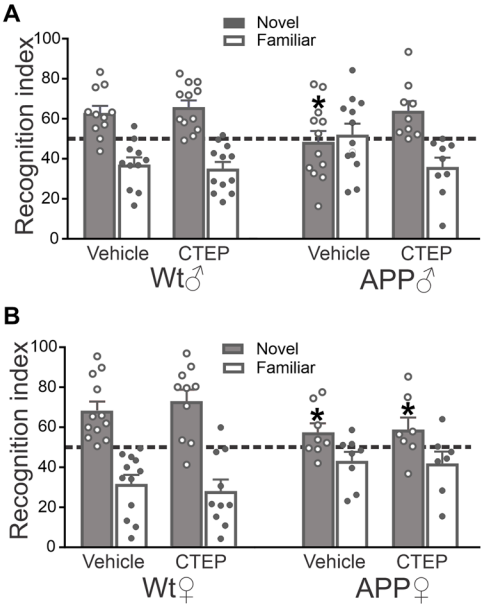

Fig. 6. CTEP improves recognition scores in male, but not in female, APP mice. (**A** and **B**) Recognition index for exploring one novel object versus familiar object in the second day of novel object recognition test after a 12-week treatment with vehicle or CTEP (2 mg/kg) of 6-month-old male (A) and female (B) Wt and APP mice. Data represents means ± SEM ($n = 8$ to 10 mice per group). Spontaneous death excluded some mice from analysis. *$P < 0.05$ versus novel object values of vehicle-treated Wt mice assessed by two-way ANOVA and Bonferroni-corrected t tests. Familiar objects' values, being the mirror of novel object values, were not compared.

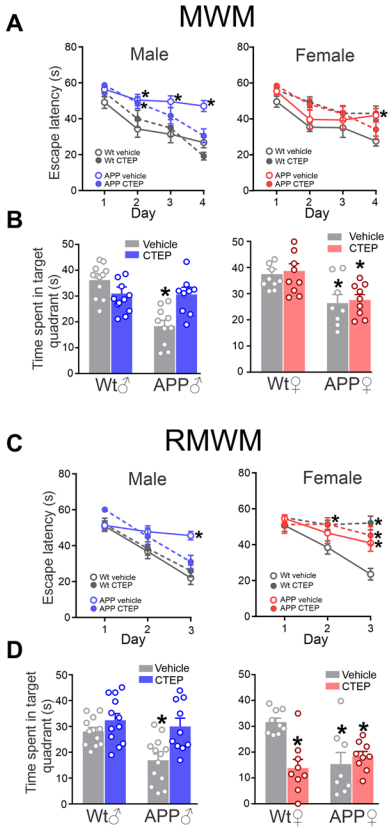

Fig. 7. CTEP treatment improves performance of male, but not female, APP mice in MWM and RMWM. (**A** to **D**) Escape latency and time spent in the target quadrant for MWM (A and B) and RMWM (C and D) in 6-month-old male and female Wt and APP mice after 12 weeks of treatment with either vehicle or CTEP (2 mg/kg). Data represent means ± SEM ($n = 8$ to 10 mice per group). Spontaneous death excluded some mice from analysis. *$P < 0.05$ versus vehicle-treated Wt assessed by two-way ANOVA and Bonferroni-corrected t tests. For escape latency, a mixed-measures ANOVA was conducted in which vehicle versus CTEP and Wt versus APP were treated as between-group measures, whereas days were treated as within-group measures.

deficits and Aβ-related pathology in males, but not in females, despite a comparable phenotype. This study has major implications as it shows how G protein–coupled receptors, the most common class of receptors targeted by prescription drugs (*38*), can exhibit distinct gender-specific pharmacological profiles that must be considered during drug development. Such insight will guide the future design of sex-tailored treatments.

The scaffolding complex formed between Aβ, PrP^C, and male mGluR5 can promote receptor clustering (*17*, *19*), prevent constitutive receptor endocytosis (*39*), and activate pathological mGluR5 signaling (*5*, *40*). One of the consequences of pathological Aβ mGluR5 activation is the inhibition of autophagy flux (*20*, *24*) triggering a feedforward mechanism leading to further accumulation of Aβ and exacerbate excitotoxicity. The binding of mGluR5 NAM CTEP to the allosteric site likely disrupts the interaction between Aβ and the receptor and consequently interrupts receptor-activated neurodegeneration in male APP mice (*20*, *24*). The lack of PrP^C/Aβ binding to female mGluR5 means that this feedforward mechanism cannot be initiated and therefore nullifies the contribution of mGluR5 to AD pathophysiology and explains the lack of mGluR5 NAM efficacy in female AD mice. Although it needs to be confirmed in future pharmacological studies, we speculate that Aβ preferentially binds to the mGluR5 allosteric site based on the ability of mGluR5 NAM to reverse Aβ-induced changes in neuronal cultures and the incomplete displacement of the radioactive ligand by Aβ. However, the latter can also be attributed to the existence of two populations of receptors that exhibit different MPEP affinities, such that mGluR5 may exist in two conformational states, with Aβ likely selectively binding to the high-affinity site, or that a less accessible MPEP binding site may exist (*41*).

Aβ oligomers are a normal proteolytic by-product of amyloid precursor protein and are present at low levels in the brain. Altered degradation of Aβ oligomers shifts the homeostasis toward increased oligomer levels and accelerates neurodegeneration (*4*, *42*). Autophagy represents an essential protein degradation pathway, and defects in autophagy are reported in the early stages of AD in animal models and patients (*43*–*47*). We find that the differential binding of Aβ to mGluR5 triggers pathological inhibition of autophagy via a ZBTB16-Cullin3-Roc1 E3-ubiquitin ligase pathway (*36*) in male, but not in female, neurons. Therefore, mGluR5 antagonism is associated with improved cognitive function, enhanced autophagy, and reduced Aβ pathology in male, but not in female, APP mice.

mGluR5-negative and silent allosteric modulators improve cognitive function in male APP mice, but only NAMs reduced Aβ oligomer–related pathology (*22*, *25*). This is of particular interest because the mGluR5 NAM basimglurant is well tolerated by patients in clinical studies for Fragile X mental retardation and major depression (*48*, *49*). These data suggest the possibility of repurposing mGluR5-selective modulators for treatment of male patients with AD. However, our findings indicate that mGluR5 contribution to AD pathophysiology in females is not significant, and the pathology

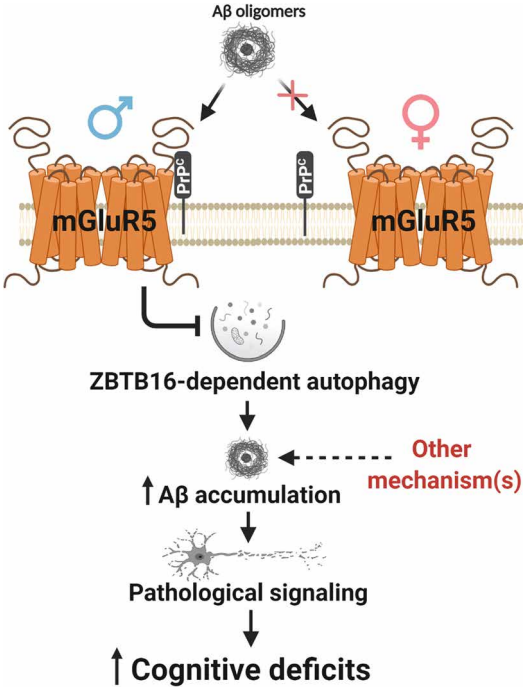

Fig. 8. Schematic representation depicting Aβ oligomer–induced sex-selective pathophysiological mGluR5 signaling. PrP^C forms a scaffolding complex with male mGluR5 and Aβ oligomers and elicits the inactivation of ZBTB16-mediated autophagy. The reduction in autophagic clearance of Aβ oligomers triggers pathological signaling and results in cognitive deficits. In female brain, lack of interaction between PrP^C and mGluR5 prevents the formation of mGluR5/Aβ oligomer/PrP^C complex, and therefore, pathological signaling and cognitive deficits are likely mediated by mGluR5-independent mechanism(s).

must be mediated by an alternative mechanism(s), thereby severely limiting the use of mGluR5 antagonists in women.

There have been no reported differences in either gene editing or genomic regulation of mGluR5 expression, subcellular localization, and/or function between both sexes. Thus, one of the major challenges of AD research remains, that is, understanding the underlying pharmacological and physiological differences in the manifestation of AD pathology in males versus females, in both animal AD mice and human patients. Although the sex-dependent regulation of the formation of the mGluR5/Aβ oligomer/PrP^C complex is clearly one of the underlying mechanisms, the biological basis for such difference in the pharmacological properties of mGluR5 between sexes remains largely unknown. mGluRs are allosterically regulated receptors, and thus, their pharmacological function may be regulated by differential interactions with either intra- or extracellular regulatory proteins in male and female animals (*16*, *50*). Our findings suggest that estrogen does not regulate Aβ/mGluR5 interaction. However, we cannot rule out sex-specific differences in mGluR5 interactomes that can alter its binding to other scaffolds such as PrP^C and Aβ. Moreover, mGluR5 is not the sole cell surface target for Aβ, and a multicity of targets can contribute to sex-dependent and sex-independent changes in synaptic signaling, autophagy, and neuronal cell death in female AD (*51*).

It is noteworthy that we detect an altered autophagy flux in female AD mice, and it will be essential to further explore the underlying signaling mechanism(s) to effectively target them. It is also possible that the role of mGluR5 in female AD mice becomes evident at advanced disease stages that warrant longitudinal studies in the future. More so, given the key role of mGluR5 in synaptic function (*5*, *52*) and the poor cognitive performance of mGluR5 NAM–treated control female mice, it will be important to exploit other aspects of altered mGluR5 synaptic signaling in the female brain.

In summary, we report that sex-specific differences in mGluR5 pharmacology observed in mouse cortical tissue are mirrored in human cortex and show that mGluR5 antagonism reduces cognitive impairment and Aβ pathology in male, but not in female, AD mice. Our data demonstrate that mGluR5 does not represent an effective pharmacological target for the treatment of AD in women, but that it remains a potentially effective target for the treatment of the early stages of AD in men.

MATERIALS AND METHODS

Reagents

CTEP (1972) was purchased from Axon Medchem. Aβ (1–42) PTD human protein (03111), the Amyloid Beta (Aggregated) Human ELISA (enzyme-linked immunosorbent assay) Kit (KHB3491), goat anti-rabbit (G-21234) and anti-mouse (G21040) immunoglobulin G (IgG; H + L) cross-adsorbed horseradish peroxidase (HRP) secondary antibody, rabbit anti-Aβ (71-5800), and rabbit anti–β-actin (PA1-183) were from Thermo Fisher Scientific. Rabbit anti–$pSer^9$-GSK3β (9323) and mouse anti-GSK3β (9832) antibodies were from Cell Signaling Technology. Rabbit anti-ATG14L (PD026) was from MBL International. Immunoprecipitation kit (206996), mouse anti-P62 (56416), rabbit anti-vinculin (129002), and rabbit anti-ZBTB16 (39354) were from Abcam. Rabbit anti-mGluR5 (AB5675) was from Millipore. Mouse Anti-Prion Protein (PrP^C) Clone SAF-32 (189720-1) was from Cayman Chemical. [^{3}H]-MPEP (VT237) was from Vitrax, and MPEP (1212) and ICI 182,780 (1047) were from Tocris. Effectene transfection reagent (301425) was from Qiagen, and VECTASTAIN Elite ABC HRP Kit (rabbit IgG, PK-6101) was from Vector Laboratories. Reagents used for Western blotting were purchased from Bio-Rad, and all other biochemical reagents were from Sigma-Aldrich.

Animals, human tissue, and mouse cells

Mice were obtained from the Jackson laboratories and bred to establish littermate controlled female and male wild type (C57BL/6J, stock# 000664), APPswe/PS1ΔE9 [B6C3-Tg (APPswe/PSEN1ΔE9)85Dbo/J, stock# 34829], and mGluR5$^{-/-}$ (B6;129-Grm5tm1Rod/J, stock# 003121) that were group housed in cages of two or more animals, received food and water ad libitum, and maintained on a 12-hour light/12-hour dark cycle at 24°C. Groups of 24 male and female wild-type and APPswe/PS1ΔE9 mice were aged to 6 months of age, and 12 mice from each group were randomized and blindly treated every 48 hours based on weekly weights with either vehicle [dimethyl sulfoxide (DMSO) in chocolate pudding] or CTEP (2 mg/kg; dissolved in 10% DMSO and then mixed with chocolate pudding; final DMSO concentration was 0.1%) for 12 weeks (*22*, *32*). Cognitive function of all animals was assessed before and after 12 weeks of drug treatment. At the end of the 12-week treatment, mice were euthanized by exsanguination, and brains were collected and randomized for biochemical determinations and immunostaining. Mice used for radioligand binding and coimmunoprecipitation experiments were 3-month-old wild type. For ICI 182,780 experiments, 3-month-old wild-type mice were injected subcutaneously daily with either ICI

182,780 (100 μg per mouse) or vehicle (ethanol/sesame oil mixture) for 2 weeks and then used for radioligand binding experiments (*53*). All animal experimental protocols were approved by the University of Ottawa Institutional Animal Care Committee and were in accordance with the Canadian Council of Animal Care guidelines.

Human tissues were obtained and collected after consent was provided by patients or the next kin in accordance with institutional review board–approved guidelines. Frozen samples of cortices from subjects under 50 years of age were acquired through the University of Alabama and the Autism Tissue Program. In addition, frozen specimens from adults above age 60 years were obtained from the Neuropathology Service at Brigham and Women's Hospital and the Department of Pathology and Laboratory Medicine at The Ottawa Hospital. Patients' gender, age, and diagnosis were as follows: male, 34 years old, vasculitis/encephalitis; male, 70 years old, dementia with Lewy bodies; male, 65 years old, dementia with Lewy bodies; male, 75 years old, healthy; female, 44 years old, carcinoma; female, 55 years old, healthy; female, 65 years old, healthy; female, 73 years old, healthy.

CF10 cells were maintained in Opti–MEM (minimum essential medium) supplemented with FBS [10% (v/v)], at 37°C in a 5% CO_2 humidified incubator. CF10 cells were transfected with FLAG-mGluR5 ± PrP^C using Effectene Transfection reagents following the manufacturer's protocol.

Primary neuronal cultures were prepared from the cortical region of E15 male and female wild-type embryo brains. Briefly, cortical tissue of each mouse embryo was trypsin digested followed by cell dissociation using a fire-polished Pasteur pipette. Cells were plated on poly-L-ornithine–coated dishes in neurobasal medium supplemented with N2 and B27 supplements, 2.0 mM GlutaMAX, penicillin (50 μg/ml), and streptomycin (50 μg/ml). Cells were maintained for 12 to 15 days at 37°C in a 5% CO_2 humidified incubator, and medium was replenishment every 4 days.

Novel object recognition test

Mice were habituated in the testing room for 30 min, and testing was blindly performed during the animal's light cycle. Mice were placed in the empty box measuring 45 × 45 × 45 cm for 5 min, and 5 min later, two identical objects were placed in the box 5 cm from the edge and 5 cm apart. Mice were returned to the box for 5 min and allowed to explore, as described previously (*32*). Time spent exploring each object was recorded using a camera fed to a computer in a separate room and analyzed using Noldus Ethovision 10 software. Mice were considered to be exploring an object if their snout was within 1 cm of the object. Each experiment was repeated 24 hours after first exposure with one object replaced with a novel object. Data were interpreted using a recognition index, as follows: time spent exploring the familiar object or the novel object over the total time spent exploring both objects multiplied by 100, and was used to measure recognition memory [TA or TB/(TA + TB)]*100, where T represents time, A represents familiar object, and B represents novel object.

MWM and RMWM tests

Animals were habituated in the testing room for 30 min, and testing was performed blindly during the animal's light cycle. The MWM test was performed in a white opaque plastic pool (120 cm in diameter), filled with water, and maintained at 25°C to prevent hypothermia, as described previously (*22*). A clear escape platform (10-cm diameter) was placed 25 cm from the perimeter and submerged 1 cm beneath the surface of the water. Visual cues were placed on the walls in the room of the maze as spatial references. Mice were trained for 4 days (four trials per day and 15 min between trails) to find the submerged platform at a fixed position from a random start point of the four equally spaced points around the pool. Each trial lasted either 60 s or until the mouse found the platform, and mice remained on the platform for 15 s before being removed to their home cage. If the mice failed to find the platform within 60 s, they were guided to the platform by the experimenter. Escape latency was measured using Ethovision 10 automated video tracking software from Noldus, and the average of four daily trials was plotted over the testing days. On day 5, the probe trial (a single trial of 60 s) was performed by removing the platform and allowing the mice to swim freely in the pool and recording the time spent in the target quadrant. The RMWM task was initiated 24 hours after completion of the MWM using the same paradigm as the MWM, with 4 days of acquisition and a probe trial. In the RMWM task, the platform was relocated to a new position, and 3 days of testing was conducted because this was sufficient to detect group differences in learning in wild-type mice.

Sandwich ELISA for Aβ oligomer levels

ELISA was performed as described previously (*22*, *24*). Briefly, brains were dissected, and one hemisphere was used to analyze oligomeric Aβ levels. Brain homogenates were divided and centrifuged at 4°C at 100,000*g* for 1 hour. The supernatant was then diluted 1:10 with kit-provided buffer before carrying out the ELISA, which was performed in triplicate and measured as detailed in the manufacturer's protocol. Protein concentrations in the homogenates were quantified using the Bradford protein assay (Bio-Rad). The final Aβ concentrations were determined after normalization to total protein levels.

Aβ immunohistochemistry

Immunostaining was performed as described previously (*22*, *24*). Briefly, brains were coronally sectioned through the cortex and hippocampus, and staining was performed on 40-μm free-floating sections using a peroxidase-based immunostaining protocol (VECTASTAIN Elite ABC HRP Kit). Sections were incubated overnight in primary antibody for Aβ (1:200) at 4°C, washed, incubated in biotinylated antibody (biotinylated horse anti-rabbit, 1:400) for 90 min at 4°C, then incubated in an avidin biotin enzyme reagent for 90 min at 4°C, and visualized using a chromogen. Sections were mounted on slides and visualized with a Zeiss AxioObserver epifluorescence microscope with a Zeiss 20× lens, using representative 900-μm^2 areas of cortex and hippocampus. Experimenters were blinded to drugging and analysis. Six to eight sections per mouse were analyzed, and for each section, five ROIs were analyzed in the cortex and two ROIs in the hippocampus using the cell counter tool in ImageJ (*54*). This number of ROIs prevents the selection of only densely stained regions.

Immunoblotting

A brain hemisphere was lysed in ice-cold lysis buffer (25 mM Hepes, 300 mM NaCl, 1.5 mM $MgCl_2$, 0.2 mM EDTA, and 1% Triton-X) containing protease inhibitor cocktail [100 μM AEBSF 4-(2-aminoethyl) benzenesulfonyl fluoride hydrochloride, 2 μM leupeptin, 80 nM aprotinin, 5 μM bestatin, 1.5 μM E-64, and 1 μM pepstatin A] and phosphatase inhibitors (10 mM NaF and 500 μM Na_3VO_4) and centrifuged twice

for 10 min each at 20,000*g* and 4°C. The supernatant was collected, and total protein levels were quantified using Bradford Protein Assay (Bio-Rad). Homogenates were diluted in a mix of lysis buffer and β-mercaptoethanol containing 3× loading buffer and boiled for 10 min at 95°C. Aliquots containing 30 to 40 μg of total proteins were resolved by electrophoresis on a 7.5 or 10% SDS–polyacrylamide gel electrophoresis (SDS-PAGE) and transferred onto nitrocellulose membranes. Blots were blocked in tris-buffered saline (pH 7.6) containing 0.05% of Tween 20 (TBST) and 5% nonfat dry milk for 1 hour at room temperature and then incubated overnight at 4°C with primary antibodies diluted 1:1000 in TBST containing 2% nonfat dry milk. Immunodetection was performed by incubating with secondary antibodies (anti-rabbit/mouse) diluted 1:5000 in TBST containing 1% of nonfat dry milk for 1 hour. Membranes were washed in TBST, and then bands were detected and quantified using SuperSignal West Pico PLUS Chemiluminescent Substrate using Bio-Rad chemiluminescence system as previously described (*32*, *55*).

Embryo sex determination for primary culture

DNA was extracted from embryonic tissue (a piece of tail) by incubation overnight at 55°C in DNA lysis buffer [50 mM tris-HCl (pH 8), 10 mM EDTA, 20 mM NaCl, and 0.031% SDS] supplemented with Proteinase K (Promega). After incubation, lysates were centrifuged at 20,000*g* for 10 min at 25°C, and the supernatant was collected. DNA was precipitated by Isopropanol and was collected by centrifugation at 10,000*g* for 10 min at 4°C. Tris-EDTA buffer [10 mM tris-HCl (pH 8) and 1 mM EDTA (pH 8)] was added to DNA, heated at 55°C for 10 min, and then used for the PCR. Primers were designed flanking an 84–base pair deletion of the X-linked *Rbm31x* gene relative to its Y-linked gametolog *Rbm31y* (forward: CACCTTAAGAACAAGCCAATACA; reverse: GGCTTGTCCTGAAAACATTTGG) (*33*). After the PCR, products were separated on an agarose gel containing RedSafe DNA stain (FroggaBio) and visualized on a Bio-Rad fluorescence system.

Primary neuronal culture experiment

After 12 to 15 days of incubation, cultures were starved in Hanks' balanced salt solution for 1 hour. Cells were then treated with 10 μM CTEP or DMSO (vehicle for CTEP) for 30 min followed by 100 nM Aβ for 1 hour at 37°C. Human Aβ oligomers were prepared as per the manufacturer's recommendations to form the neurotoxic aggregates (*56*). After this treatment, neuronal cultures were lysed with ice-cold radioimmunoprecipitation assay buffer [RIPA; 150 mM NaCl, 5 mM EDTA, 25 mM tris-HCl (pH 7.4), 1% NP-40, 0.5% sodium deoxycholate, and 0.1% SDS] buffer supplemented with protease and phosphatase inhibitors described above, and then immunoblotting was performed.

Radioligand binding

Radioligand binding was performed as previously described (*57*). Briefly, cells washed with phosphate-buffered saline and ice-cold lysis buffer [10 mM tris-HCl (pH 7.4) and 5 mM EDTA (pH 8.0)] were used to detach the cells. Cortices from mice and human were homogenized in ice-cold lysis buffer. To prepare the crude membrane preparation, cell or brain lysates were centrifuged twice at 40,000*g* for 20 min at 4°C, supernatant was discarded after each centrifugation, and the pellets were resuspended in lysis buffer. The crude membrane preparations were then suspended in resuspension buffer [62.5 mM tris-HCl (pH 7.4) and 1.25 mM EDTA (pH 8.0)] and kept on ice. The binding reactions were performed in duplicate by incubating crude membranes with 3 nM [^{3}H]-MPEP and increasing concentrations of either MPEP or Aβ oligomers in binding buffer [62.5 mM tris-HCl (pH 7.4) and 1.25 mM EDTA (pH 8.0), 200 mM NaCl, 6.7 mM $MgCl_2$, 2.5 mM $CaCl_2$, and 8.33 mM KCl] at room temperature for 90 min. The nonspecific binding was determined using 10 μM MPEP. The binding reactions were terminated by rapid filtration through Whatman GF/C glass fiber filter sheets using a semiautomated harvesting system (Brandel). The tritium-bound radioactivity was then counted using a liquid scintillation counter (Beckman). The data were analyzed using GraphPad Prism, [^{3}H]-MPEP binding as percentage of maximum specific binding was calculated, and the equilibrium dissociation constant (K_i, M) of MPEP and Aβ was determined.

Coimmunoprecipitation

Hippocampus from male and female wild-type and mGluR5$^{-/-}$ mice was dissected and lysed in nondenaturing lysis buffer containing protease inhibitors provided with coimmunoprecipitation kit (Abcam; 206996). Lysates were rotated for 1 hour at 4°C and centrifuged at 10,000*g* for 10 min at 4°C to pellet insoluble material. Precleared supernatant (500 μg) was incubated with 1 μg of anti-PrP^C antibody overnight at 4°C. Freshly washed protein A/G sepharose beads were added to lysate/antibody mixture, and samples were rotated for 2 hours at 4°C. Beads were washed with wash buffer provided in the kit and then boiled with 3× loading buffer containing β-mercaptoethanol for 10 min at 90°C. Samples were separated by SDS-PAGE and immunoblotted to identify coimmunoprecipitated mGluR5. An additional immunoblot was performed to examine mGluR5 and PrP^C protein expression in lysates prepared before incubation with antibody.

Statistical analysis

Means ± SEM are shown for each of independent experiments shown in the various figure legends. GraphPad Prism 8 was used to analyze data for normality and statistical significance. Data normality was tested using Anderson-Darling and D'Agostino-Pearson omnibus tests, statistical significance was determined by two-way or three-way analyses of variance (ANOVAs), and Bonferroni-corrected *t* tests, Fisher's least significant difference (LSD), or Kruskal-Wallis tests were used to determine the source of significant interactions. Statistical details of individual experiments are indicated in the figure legends.

SUPPLEMENTARY MATERIALS

stke.sciencemag.org/cgi/content/full/13/662/eabd2494/DC1

Fig. S1. Individual blots used for quantification presented in Fig. 2C.

Fig. S2. Individual blots used for quantification presented in Fig. 4B.

Fig. S3. Individual blots used for quantification presented in Fig. 5 (A to D).

Table S1. Maximum specific binding and calculated K_i values for binding curves in Figs. 1 and 3.

View/request a protocol for this paper from *Bio-protocol*.

REFERENCES AND NOTES

1. L. Rizzi, I. Rosset, M. Roriz-Cruz, Global epidemiology of Dementia: Alzheimer's and vascular types. *Biomed. Res. Int.* **2014**, 908915 (2014).
2. D. A. Casey, D. Antimisiaris, J. O'Brien, Drugs for Alzheimer's disease: Are they effective? *P. T.* **35**, 208–211 (2010).
3. K. L. Lanctôt, R. D. Rajaram, N. Herrmann, Therapy for Alzheimer's disease: How effective are current treatments? *Ther. Adv. Neurol. Disord.* **2**, 163–180 (2009).
4. S. Hunter, C. Brayne, Understanding the roles of mutations in the amyloid precursor protein in Alzheimer disease. *Mol. Psychiatry* **23**, 81–93 (2018).

5. A. Hamilton, G. W. Zamponi, S. S. G. Ferguson, Glutamate receptors function as scaffolds for the regulation of β-amyloid and cellular prion protein signaling complexes. *Mol. Brain* **8**, 18 (2015).
6. J. C. Polanco, C. Li, L.-G. Bodea, R. Martinez-Marmol, F. A. Meunier, J. Götz, Amyloid-β and tau complexity – towards improved biomarkers and targeted therapies. *Nat. Rev. Neurol.* **14**, 22–39 (2018).
7. J. L. Podcasy, C. N. Epperson, Considering sex and gender in Alzheimer disease and other dementias. *Dialogues Clin. Neurosci.* **18**, 437–446 (2016).
8. D. W. Fisher, D. A. Bennett, H. Dong, Sexual dimorphism in predisposition to Alzheimer's disease. *Neurobiol. Aging* **70**, 308–324 (2018).
9. R. S. Vest, C. J. Pike, Gender, sex steroid hormones, and Alzheimer's disease. *Horm. Behav.* **63**, 301–307 (2013).
10. H. Hampel, A. Vergallo, F. S. Giorgi, S. H. Kim, H. Depypere, M. Graziani, A. Saidi, R. Nisticò, S. Lista; Alzheimer Precision Medicine Initiative (APMI), Precision medicine and drug development in Alzheimer's disease: The importance of sexual dimorphism and patient stratification. *Front. Neuroendocrinol.* **50**, 31–51 (2018).
11. K. R. Laws, K. Irvine, T. M. Gale, Sex differences in cognitive impairment in Alzheimer's disease. *World J. Psychiatry* **6**, 54–65 (2016).
12. Y. Tang, Z. Min, X.-J. Xiang, L. Liu, Y.-L. Ma, B.-L. Zhu, L. Song, J. Tang, X.-J. Deng, Z. Yan, G.-J. Chen, Estrogen-related receptor alpha is involved in Alzheimer's disease-like pathology. *Exp. Neurol.* **305**, 89–96 (2018).
13. J. F. Kelly, J. F. Kelly, J. L. Bienias, A. Shah, K. A. Meeke, J. A. Schneider, E. Soriano, D. A. Bennett, Levels of estrogen receptors α and β in frontal cortex of patients with Alzheimer's disease: Relationship to mini-mental state examination scores. *Curr. Alzheimer Res.* **5**, 45–51 (2008).
14. S. R. Rapp, M. A. Espeland, S. A. Shumaker, V. W. Henderson, R. L. Brunner, J. A. E. Manson, M. L. S. Gass, M. L. Stefanick, D. S. Lane, J. Hays, K. C. Johnson, L. H. Coker, M. Dailey, D. Bowen; WHIMS Investigators, Effect of estrogen plus progestin on global cognitive function in postmenopausal women: The Women's Health Initiative Memory Study: A randomized controlled trial. *JAMA* **289**, 2663–2672 (2003).
15. A. C. McCarrey, S. M. Resnick, Postmenopausal hormone therapy and cognition. *Horm. Behav.* **74**, 167–172 (2015).
16. C. M. Niswender, P. J. Conn, Metabotropic glutamate receptors: Physiology, pharmacology, and disease. *Annu. Rev. Pharmacol. Toxicol.* **50**, 295–322 (2010).
17. J. W. Um, A. C. Kaufman, M. Kostylev, J. K. Heiss, M. Stagi, H. Takahashi, M. E. Kerrisk, A. Vortmeyer, T. Wisniewski, A. J. Koleske, E. C. Gunther, H. B. Nygaard, S. M. Strittmatter, Metabotropic glutamate receptor 5 is a coreceptor for Alzheimer Aβ oligomer bound to cellular prion protein. *Neuron* **79**, 887–902 (2013).
18. L. T. Haas, M. A. Kostylev, S. M. Strittmatter, Therapeutic molecules and endogenous ligands regulate the interaction between brain cellular prion protein (PrP^C) and metabotropic glutamate receptor 5 (mGluR5). *J. Biol. Chem.* **289**, 28460–28477 (2014).
19. M. Renner, P. N. Lacor, P. T. Velasco, J. Xu, A. Contractor, W. L. Klein, A. Triller, Deleterious effects of amyloid β oligomers acting as an extracellular scaffold for mGluR5. *Neuron* **66**, 739–754 (2010).
20. K. S. Abd-Elrahman, A. Hamilton, M. Vasefi, S. S. G. Ferguson, Autophagy is increased following either pharmacological or genetic silencing of mGluR5 signaling in Alzheimer's disease mouse models. *Mol. Brain* **11**, 19 (2018).
21. A. Hamilton, J. L. Esseltine, R. A. DeVries, S. P. Cregan, S. S. G. Ferguson, Metabotropic glutamate receptor 5 knockout reduces cognitive impairment and pathogenesis in a mouse model of Alzheimer's disease. *Mol. Brain* **7**, 40 (2014).
22. A. Hamilton, M. Vasefi, C. Vander Tuin, R. J. Mcquaid, H. Anisman, S. S. G. Ferguson, Chronic pharmacological mGluR5 inhibition prevents cognitive impairment and reduces pathogenesis in an Alzheimer disease mouse model. *Cell Rep.* **15**, 1859–1865 (2016).
23. D. Zhang, Y. Qi, I. Klyubin, T. Ondrejcak, C. J. Sarell, A. C. Cuello, J. Collinge, M. J. Rowan, Targeting glutamatergic and cellular prion protein mechanisms of amyloid β-mediated persistent synaptic plasticity disruption: Longitudinal studies. *Neuropharmacology* **121**, 231–246 (2017).
24. K. S. Abd-Elrahman, A. Hamilton, A. Albaker, S. S. G. Ferguson, mGluR5 contribution to neuropathology in Alzheimer mice is disease stage-dependent. *ACS Pharmacol. Transl. Sci.* **3**, 334–344 (2020).
25. L. T. Haas, S. V. Salazar, L. M. Smith, H. R. Zhao, T. O. Cox, C. S. Herber, A. P. Degnan, A. Balakrishnan, J. E. Macor, C. F. Albright, S. M. Strittmatter, Silent allosteric modulation of mGluR5 maintains glutamate signaling while rescuing Alzheimer's mouse phenotypes. *Cell Rep.* **20**, 76–88 (2017).
26. P. M. Q. Bellozi, G. F. Gomes, M. C. M. Silva, I. V. de Assis Lima, C. R. Á. Batista, W. de Oliveira Carneiro Junior, J. G. Dória, É. L. M. Vieira, R. P. Vieira, R. P. Freitas, C. N. Ferreira, E. Candelario-Jalil, T. Wyss-Coray, F. M. Ribeiro, A. C. P. Oliveira, A positive allosteric modulator of mGluR5 promotes neuroprotective effects in mouse models of Alzheimer's disease. *Neuropharmacology* **160**, 107785 (2019).
27. L. Lindemann, G. Jaeschke, A. Michalon, E. Vieira, M. Honer, W. Spooren, R. Porter, T. Hartung, S. Kolczewski, B. Büttelmann, C. Flament, C. Diener, C. Fischer, S. Gatti, E. P. Prinssen, N. Parrott, G. Hoffmann, J. G. Wettstein, CTEP: A novel, potent, long-acting, and orally bioavailable metabotropic glutamate receptor 5 inhibitor. *J. Pharmacol. Exp. Ther.* **339**, 474–486 (2011).
28. J. L. Jankowsky, D. J. Fadale, J. Anderson, G. M. Xu, V. Gonzales, N. A. Jenkins, N. G. Copeland, M. K. Lee, L. H. Younkin, S. L. Wagner, S. G. Younkin, D. R. Borchelt, Mutant presenilins specifically elevate the levels of the 42 residue β-amyloid peptide in vivo: Evidence for augmentation of a 42-specific γ secretase. *Hum. Mol. Genet.* **13**, 159–170 (2004).
29. N.-W. Hu, A. J. Nicoll, D. Zhang, A. J. Mably, T. O'Malley, S. A. Purro, C. Terry, J. Collinge, D. M. Walsh, M. J. Rowan, mGlu5 receptors and cellular prion protein mediate amyloid-β-facilitated synaptic long-term depression in vivo. *Nat. Commun.* **5**, 3374 (2014).
30. L. T. Haas, S. M. Strittmatter, Oligomers of amyloid prevent physiological activation of the cellular prion protein-metabotropic glutamate receptor 5 complex by glutamate in Alzheimer disease. *J. Biol. Chem.* **291**, 17112–17121 (2016).
31. F. H. Beraldo, V. G. Ostapchenko, F. A. Caetano, A. L. S. Guimaraes, G. D. S. Ferretti, N. Daude, L. Bertram, K. O. P. C. Nogueira, J. L. Silva, D. Westaway, N. R. Cashman, V. R. Martins, V. F. Prado, M. A. M. Prado, Regulation of amyloid β oligomer binding to neurons and neurotoxicity by the prion protein-mGluR5 complex. *J. Biol. Chem.* **291**, 21945–21955 (2016).
32. K. S. Abd-Elrahman, A. Hamilton, S. R. Hutchinson, F. Liu, R. C. Russell, S. S. G. Ferguson, mGluR5 antagonism increases autophagy and prevents disease progression in the *zQ175* mouse model of Huntington's disease. *Sci. Signal.* **10**, eaan6387 (2017).
33. S. J. Tunster, Genetic sex determination of mice by simplex PCR. *Biol. Sex Differ.* **8**, 31 (2017).
34. L. Ruan, Z. Kang, G. Pei, Y. Le, Amyloid deposition and inflammation in APPswe/PS1dE9 mouse model of Alzheimer's disease. *Curr. Alzheimer Res.* **6**, 531–540 (2009).
35. J. Wang, H. Tanila, J. Puoliväli, I. Kadish, T. van Groen, Gender differences in the amount and deposition of amyloidβ in APPswe and PS1 double transgenic mice. *Neurobiol. Dis.* **14**, 318–327 (2003).
36. T. Zhang, K. Dong, W. Liang, D. Xu, H. Xia, J. Geng, A. Najafov, M. Liu, Y. Li, X. Han, J. Xiao, Z. Jin, T. Peng, Y. Gao, Y. Cai, C. Qi, Q. Zhang, A. Sun, M. Lipinski, H. Zhu, Y. Xiong, P. P. Pandolfi, H. Li, Q. Yu, J. Yuan, G-protein-coupled receptors regulate autophagy by ZBTB16-mediated ubiquitination and proteasomal degradation of Atg14L. *eLife* **4**, e06734 (2015).
37. A. Krishnankutty, T. Kimura, T. Saito, K. Aoyagi, A. Asada, S.-I. Takahashi, K. Ando, M. Ohara-Imaizumi, K. Ishiguro, S.-i. Hisanaga, *In vivo* regulation of glycogen synthase kinase 3β activity in neurons and brains. *Sci. Rep.* **7**, 8602 (2017).
38. P. A. Insel, C.-M. Tang, I. Hahntow, M. C. Michel, Impact of GPCRs in clinical medicine: Monogenic diseases, genetic variants and drug targets. *Biochim. Biophys. Acta* **1768**, 994–1005 (2007).
39. F. Raka, A. R. Di Sebastiano, S. C. Kulhawy, F. M. Ribeiro, C. M. Godin, F. A. Caetano, S. Angers, S. S. G. Ferguson, Ca^{2+}/calmodulin-dependent protein kinase II interacts with group i metabotropic glutamate and facilitates receptor endocytosis and ERK1/2 signaling: Role of β-amyloid. *Mol. Brain* **8**, 21 (2015).
40. L. T. Haas, S. V. Salazar, M. A. Kostylev, J. W. Um, A. C. Kaufman, S. M. Strittmatter, Metabotropic glutamate receptor 5 couples cellular prion protein to intracellular signalling in Alzheimer's disease. *Brain* **139**, 526–546 (2016).
41. D. Guo, L. A. Peletier, L. Bridge, W. Keur, H. de Vries, A. Zweemer, L. H. Heitman, A. P. IJzerman, A two-state model for the kinetics of competitive radioligand binding. *Br. J. Pharmacol.* **175**, 1719–1730 (2018).
42. R. J. O'Brien, P. C. Wong, Amyloid precursor protein processing and Alzheimer's disease. *Annu. Rev. Neurosci.* **34**, 185–204 (2011).
43. J. Nah, J. Yuan, Y.-K. Jung, Autophagy in neurodegenerative diseases: From mechanism to therapeutic approach. *Mol. Cells* **38**, 381–389 (2015).
44. R. A. Nixon, The role of autophagy in neurodegenerative disease. *Nat. Med.* **19**, 983–997 (2013).
45. Q. Li, Y. Liu, M. Sun, Autophagy and Alzheimer's disease. *Cell. Mol. Neurobiol.* **37**, 377–388 (2017).
46. M. E. Orr, S. Oddo, Autophagic/lysosomal dysfunction in Alzheimer's disease. *Alzheimers. Res. Ther.* **5**, 53 (2013).
47. D. C. Rubinsztein, M. D. Figlia, N. Heintz, R. A. Nixon, Z.-H. Qin, B. Ravikumar, L. Stefanis, A. Tolkovsky, Autophagy and its possible roles in nervous system diseases, damage and repair. *Autophagy* **1**, 11–22 (2005).
48. J. A. Quiroz, P. Tamburri, D. Deptula, L. Banken, U. Beyer, M. Rabbia, N. Parkar, P. Fontoura, L. Santarelli, Efficacy and safety of basimglurant as adjunctive therapy for major depression: A randomized clinical trial. *JAMA Psychiat.* **73**, 675–684 (2016).
49. E. A. Youssef, E. Berry-Kravis, C. Czech, R. J. Hagerman, D. Hessl, C. Y. Wong, M. Rabbia, D. Deptula, A. John, R. Kinch, P. Drewitt, L. Lindemann, M. Marcinowski, R. Langland, C. Horn, P. Fontoura, L. Santarelli, J. A. Quiroz; FragXis Study Group, Effect of the mGluR5-NAM basimglurant on behavior in adolescents and adults with fragile X syndrome in a randomized, double-blind, placebo-controlled trial: FragXis phase 2 results. *Neuropsychopharmacology* **43**, 503–512 (2018).

50. H. A. Dunn, C. Orlandi, K. A. Martemyanov, Beyond the ligand: Extracellular and transcellular G protein–coupled receptor complexes in physiology and pharmacology. *Pharmacol. Rev.* **71**, 503–519 (2019).
51. G.-f. Chen, T.-h. Xu, Y. Yan, Y.-r. Zhou, Y. Jiang, K. Melcher, H. E. Xu, Amyloid beta: Structure, biology and structure-based therapeutic development. *Acta Pharmacol. Sin.* **38**, 1205–1235 (2017).
52. T. M. Piers, D. H. Kim, B. C. Kim, P. Regan, D. J. Whitcomb, K. Cho, Translational concepts of mglur5 in synaptic diseases of the brain. *Front. Pharmacol.* **3**, 199 (2012).
53. M. Sawada, N. J. Alkayed, S. Goto, B. J. Crain, R. J. Traystman, A. Shaivitz, R. J. Nelson, P. D. Hurn, Estrogen receptor antagonist ICI182,780 exacerbates ischemic injury in female mouse. *J. Cereb. Blood Flow Metab.* **20**, 112–118 (2000).
54. C. A. Schneider, W. S. Rasband, K. W. Eliceiri, NIH Image to ImageJ: 25 years of image analysis. *Nat. Methods* **9**, 671–675 (2012).
55. K. Farmer, K. S. Abd-Elrahman, A. Derksen, E. M. Rowe, A. M. Thompson, C. A. Rudyk, N. A. Prowse, Z. Dwyer, S. C. Bureau, T. Fortin, S. S. G. Ferguson, S. Hayley, mGluR5 allosteric modulation promotes neurorecovery in a 6-OHDA-toxicant model of parkinson's disease. *Mol. Neurobiol.* **57**, 1418–1431 (2020).
56. L. K. Simmons, P. C. May, K. J. Tomaselli, R. E. Rydel, K. S. Fuson, E. F. Brigham, S. Wright, I. Lieberburg, G. W. Becker, D. N. Brems, W. Y. Li, Secondary structure of amyloid β peptide correlates with neurotoxic activity in vitro. *Mol. Pharmacol.* **45**, 373–379 (1994).
57. B. Plouffe, M. Tiberi, Functional analysis of human D1 and D5 dopaminergic G protein-coupled receptors: Lessons from mutagenesis of a conserved serine residue in the cytosolic end of transmembrane region 6. *Methods Mol. Biol.* **964**, 141–180 (2013).

Acknowledgments: K.S.A.-E. is a Lecturer at the Department of Pharmacology and Toxicology, Faculty of Pharmacy, Alexandria University. We thank S. Hutchinson for breeding the mouse colony; the Behavior and Physiology core at the University of Ottawa for assistance; B. Albraidy for technical assistance; S. Priola (NIH) for providing the CF10 cells; A. West (Duke University), J. Chan (University Calgary), and J. Woulfe (The Ottawa Hospital) for assistance in procuring human tissues; and H. Anisman (Carleton University) for assistance in the statistical analysis. Figure 8 was created using BioRender.com. **Funding:** S.S.G.F is a Tier I Canada Research Chair in Brain and Mind. This study was supported by Canadian Institutes for Health Research (CIHR) grants (PJT-148656 and PJT-165967), Funding from the Krembil Foundation and the University of Ottawa and the Shanghai Institute of Materia Medica (SIMM-uOttawa) Joint Research Center to S.S.G.F., and a Clinician Postdoctoral Fellowship from the Alberta Innovates Health Solutions (AIHS) and CIHR to K.S.A.-E. **Author contributions:** K.S.A.-E., A.H., and S.S.G.F. conceptualized the study. K.S.A.-E., A.A., J.M.d.S., and A.H. optimized the methodology and performed the formal analysis and investigation. F.M.R., M.G.S., M.T., and S.S.G.F. provided resources. K.S.A.-E. wrote the original draft and, with S.S.G.F., revised the final version. S.S.G.F. supervised the study and acquired the funding. **Competing interests:** The authors declare that they have no competing interests. **Data and materials availability:** All data needed to evaluate the conclusions in the paper are present in the paper or the Supplementary Materials.

Submitted 10 June 2020
Accepted 3 November 2020
Published 15 December 2020
10.1126/scisignal.abd2494

Citation: K. S. Abd-Elrahman, A. Albaker, J. M. de Souza, F. M. Ribeiro, M. G. Schlossmacher, M. Tiberi, A. Hamilton, S. S. G. Ferguson, Aβ oligomers induce pathophysiological mGluR5 signaling in Alzheimer's disease model mice in a sex-selective manner. *Sci. Signal.* **13**, eabd2494 (2020).

Science Signaling

Aβ oligomers induce pathophysiological mGluR5 signaling in Alzheimer's disease model mice in a sex-selective manner

Khaled S. Abd-Elrahman, Awatif Albaker, Jessica M. de Souza, Fabiola M. Ribeiro, Michael G. Schlossmacher, Mario Tiberi, Alison Hamilton and Stephen S. G. Ferguson

Sci. Signal. **13** (662), eabd2494.
DOI: 10.1126/scisignal.abd2494

Men only for an Alzheimer's drug target

β-Amyloid (Aβ) deposits in the brain contribute to the progression of Alzheimer's disease (AD) by inducing excitotoxic signaling in neurons. A β binds to the metabotropic glutamate receptor mGluR5, and pharmacological inhibition of mGluR5 reverses cognitive decline in male AD model animals. However, Abd-Elrahman *et al.* found that Aβ bound to mGluR5 in postmortem brain tissue only from male AD model mice and male human donors. This sex-selective interaction was mediated by prion protein in male mouse brain tissue. The findings suggest that mGluR5 inhibitors may be therapeutically beneficial only for male patients with AD.

Science Signaling (ISSN 1937-9145) is published by the American Association for the Advancement of Science, 1200 New York Avenue NW, Washington, DC 20005. The title *Science Signaling* is a registered trademark of AAAS.